ELSEVIER

Chemical Engineering Journal 85 (2002) 127–135

Chemical Engineering Journal

www.elsevier.com/locate/cej

Continuous deionization of a dilute nickel solution

P.B. Spoor [a,*], L. Koene [a], W.R. ter Veen [b], L.J.J. Janssen [a]

[a] *Laboratory of Process Development, Department of Chemical Engineering, Eindhoven University of Technology, PO Box 513, 5600 MB Eindhoven, The Netherlands*

[b] *TNO Institute of Environmental Sciences, Energy Research and Process Innovation, Laan van Westenenk 501, PO Box 342, 7300 AH Apeldoorn, The Netherlands*

Received 21 December 2000; accepted 19 March 2001

Abstract

This paper describes the continuous removal of nickel ions from a dilute solution using a hybrid ion-exchange/electrodialysis process. Emphasis was placed on the ionic state of the bed during the process, and the mass balance of ions in the system. Much of this information was obtained by analysing the current distribution across the cell. The effects of temperature, feed nickel concentration and feed solution flow rate were ascertained. It was found that a steady, continuous process can be achieved.

Keywords: Deionization; Electrodialysis; Ion-exchange; Nickel ions

1. Introduction

The combination of electrodialysis and ion-exchange particles for the removal of ions from solution has received a great deal of attention. One of the first to mention such a combination, in this case for the treatment of radioactive wastes, was Glueckauf [1]. Much of the work, however, has been focused on the removal of monovalent ions and the production of ultra-pure water [2–6], while the removal of bivalent ions has been studied to a lesser degree [7–10]. This work follows previous studies involved in the treatment of dilute nickel solutions; parameters such as the fraction of nickel in the packed bed [11], the potential difference over the bed [12], bed width [11,12], concentration of nickel ions in the feed solution and the migration rate of the nickel front through the bed at various bed voltages [12] were examined. This paper will focus on the long-term behaviour of the combined process. The studies were carried out for up to 100 h and involved variations in the feed flow rate, temperature and the concentration of the nickel feed. These parameters are important as they may affect the nickel flux and current efficiency of the process. The purpose is to design a continuous deionization system for the removal of various heavy metals from process solutions of low concentration.

The process involves a bed of ion-exchange particles placed between two ion-selective membranes. The nickel from the feed solution will be absorbed by the particles and migrate under a potential gradient to the cathode. The system can be described in two ways: either as an ion-exchange column continuously regenerated by the application of a potential gradient perpendicular to the column length or as an electrodialysis system whose conductivity and selectivity is aided by the presence of a packed bed of ion-exchange particles in the dilute compartment.

2. Experimental

The experimental set-up has been previously described in [12]. It consisted of a three-compartment cell with an effective area of 50 cm^2 (1 cm wide × 50 cm long) (Fig. 1). The outer compartments contained the electrodes and were each connected to separate 1 M H_2SO_4 electrolyte circuits. The centre compartment contained a packed bed of ion-exchange particles (Dowex 50X-2 50-100 mesh) initially in the H^+ form, while two Nafion 117 cation-selective membranes were used to separate the three compartments. Various $NiSO_4$ feed solutions were fed through the centre compartment top-down.

The electrodes were comprised of 20 separate platinum segments that were 0.024 m in height, 0.010 m in width and separated by a distance of 0.001 m. Each electrode

* Corresponding author.
E-mail address: p.b.spoor@tue.nl (P.B. Spoor).

1385-8947/02/$ – see front matter
PII: S1385-8947(01)00216-9

Nomenclature

A	area of the bed perpendicular to nickel migration (m)
ΔE	cell voltage (V)
H	bed position measured from top of the cell (m)
n_i	quantity of species i (mol)
N_i	flux of species i (mol m^{-2} s^{-1})
t	time (s)
v	feed solution flow rate (cm^3 s^{-1})

Subscripts

a	anode compartment
b	base of nickel front
bed	bed of ion-exchange resin occupying centre compartment
cell	entire cell including anode, cathode and centre compartments
eff	centre compartment effluent solution
feed	feed solution
k	cathode compartment
t	tip of nickel front

pair was connected to a separate channel of a potentiostat. Segment-1 was located at the top of the cell where the feed solution was introduced, while segment-20 was located at the bottom, or exit, of the cell. This set-up allowed for an accurate determination of the current distribution down the column during operation at a constant cell voltage. Other measurements included the temperature along the column (Pt-100 thermocouples inserted into the wall of the centre compartment), and the pH and conductivity of the processed solution. These data were recorded continuously with the aid of a computer. Mass transport information was acquired by analysing the nickel contents in the catholyte, processed effluent solution and anolyte. Regular sampling of these solutions and subsequent analysis of the samples by either Flame AAS or UV/Vis spectroscopy, depending on concentration, were carried out. The pressure drop across the cell as well as the position of the nickel front, measured from the top of the cell, was measured periodically.

The experiments follow the same procedure as described in [12] with a few changes to the experimental parameters. These parameters are given in Table 1.

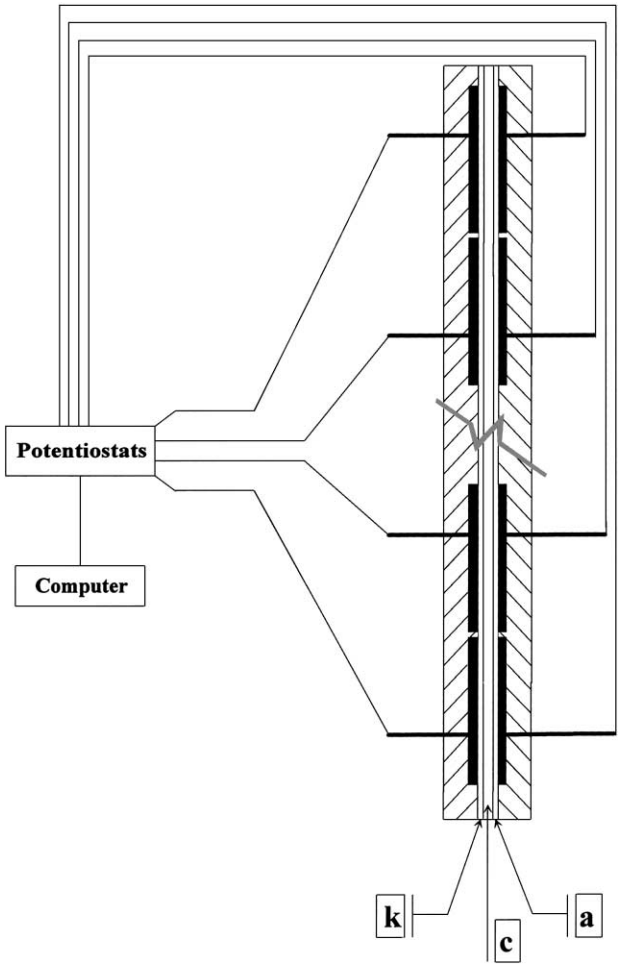

Fig. 1. Section of the segmented electrode cell depicting the anode (a), cathode (k), and centre (c) compartments.

3. Results

3.1. Experiment 1: initial experiment

In this experiment, all parameters mentioned in Table 1, aside from the temperature, were held constant. This experiment was carried out to determine if the process would reach a steady state during its 110 h duration. During the week-long experiment, it was found that changes in the ambient temperature affected the temperature in the cell; this will be discussed in more detail below.

Table 1
Experimental parameters

Experiment	Cell voltage (V)	Feed Ni^{2+} concentration (mM)	Feed flow rate (cm^3 s^{-1})	Electrolyte and feed temperature (°C)
1	5	1	0.53	25 initial
2	5	2	0.53	Incremented: 25, 30, 35, 40
3	5	1	Incremented: 0.25, 0.38, 0.58, 0.8, 0.92	25

When the 1 mM $NiSO_4$ feed solution was introduced to the centre compartment, the Ni^{2+} ions were absorbed by the ion-exchanger. This caused the bed to turn from its original yellow colour when in the hydrogen form to the dark green colour indicative of its nickel form. A clear yellow/green boundary, or front, resulted (Fig. 2). This front was observed to move down the bed.

As the front moved down the column it was also observed to change in shape; it became less flat and more elongated along the cathode side of the cell. The resulting *tip* and *base* of the front is indicated in Fig. 2. The position of the front in the column was not constant over the course of the experiment. It was observed to retreat and advance on a daily basis, hovering around an average position. A sharp decrease in particle volume occurred upon the conversion of the particles from the hydrogen to nickel form [12,13]. This caused the bed to contract, leaving the first three segment pairs without an adjacent resin bed.

The current that passed through the various electrode pairs for the first 80 h of this experiment is given in Fig. 3 as a function of time. For clarity, only the channels involved in exchange with Ni^{2+} are given. The position of the nickel front can be determined from the current distribution. This is possible due to the large mobility difference between the divalent nickel ion and the hydrogen ion in the system [13]. When the current across a pair of segments was relatively high the bed between the segments was in the hydrogen form. A low current across a pair of segments corresponded to a section of the bed in the nickel form. It was found that when the tip of the front reached the top of a segment, its current began to decrease. This current stabilized when the base of the front reached the bottom of the segment pair. It can be seen that the current across a number of the segment

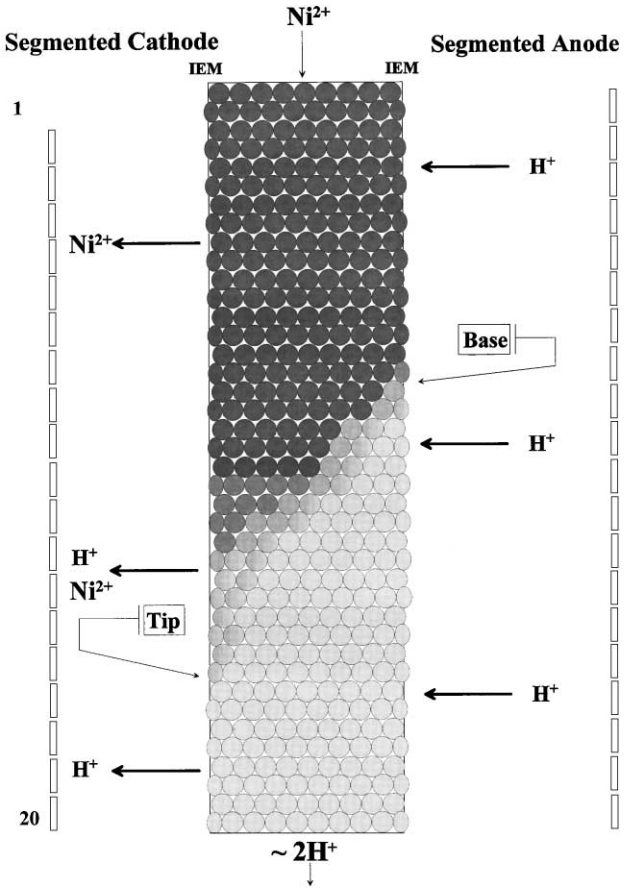

Fig. 2. Diagram of the nickel front. This figure depicts the sections of the bed in the Ni^{2+}, H^+ and Ni^{2+}/H^+ forms. The bed is regenerated by H^+ supplied by the anolyte, while nickel is concentrated in the cathode compartment. The nickel solution is fed top-down.

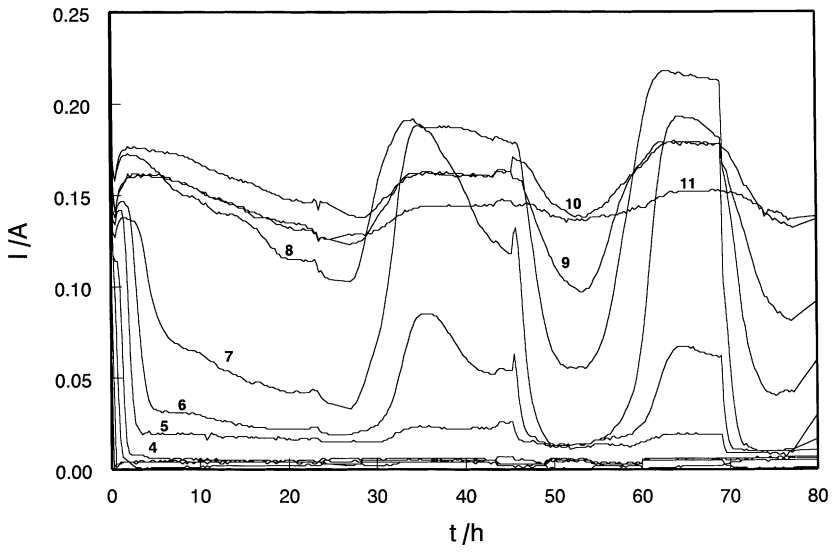

Fig. 3. Current distribution for the first 80 h of experiment 1. The first 11 channels, representing a bed position of 27.5 cm, are depicted. A cell voltage of 5 V was applied. The current across the remaining portion of the bed remained relatively constant at currents between 0.15 and 0.25 A. During the first 24 h, the current across the segments decreases in consecutive order.

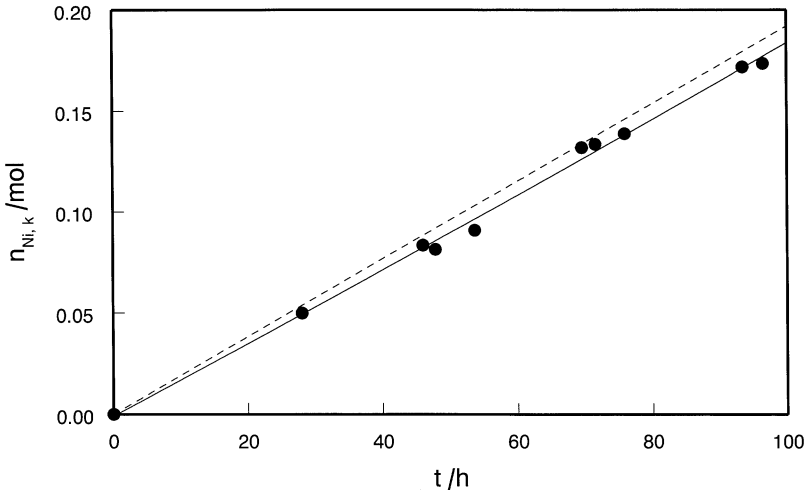

Fig. 4. Quantity of nickel transported to the cathode compartment (●) and the total amount of nickel introduced to the cell during experiment 1 (dashed line). The $NiSO_4$ feed had a concentration of 1 mM and a flow rate of 0.53 $cm^3\,s^{-1}$. A cell voltage of 5 V was applied.

pairs (segments 10–16) was not stable, but oscillated periodically.

The total amount of nickel introduced to the cell and the amount transported into the cathode compartment is shown in Fig. 4 as a function of time. This figure shows that the flux of nickel into the cathode compartment was relatively constant over the entire experiment. Only a small difference between the amount of nickel entering the cell and the amount removed from the bed was observed. The amount of nickel in the effluent of the centre compartment was below the detection limit (~20 ppb) of the AAS instrument used for the analysis. The effluent pH during the experiment averaged 2.65, this corresponds to a H^+ concentration of 2.24 mM.

The formation of a green $Ni(OH)_2$ deposit in the centre compartment, the occurrence of which was observed in previous experiments yet to be published, was not observed in this case.

3.2. Experiment 2: temperature variation

The temperature of the system affects the conductivity, and hence the ionic fluxes in the bed. Its effect on the system was, therefore, studied. This experiment was carried out over a period of 90 h at various temperatures and a nickel feed concentration of 2 mM. This higher feed concentration was used in order to: (a) utilize a greater portion of the cell than that used in experiment 1 (i.e. resulting in a larger region of the bed in the nickel form); (b) observe any other consequences it may have.

During the first 24 h the experiment was run at 25 °C. During this time, the nickel front was observed to exit the cell at the bottom of the packed bed. This was due to the increased quantity of nickel fed into the cell. The formation of $Ni(OH)_2$ in the centre compartment was observed after approximately 6 h of operation. It formed as dendrites on the cathode side membrane in the top 0.1 m of the cell. Nickel hydroxide dendrite formation occurred on this section of membrane, because due to bed contraction, it did not have an adjacent bed of particles.

Along the cathode cation-selective membrane, precipitate was also observed as non-uniform patches in the bed. Precipitate only formed in areas of the bed in the nickel form. Due to the absence of ion-exchange particles adjacent to segment pairs 1–4, these segments were turned off at $t = 30$ h to prevent further $Ni(OH)_2$ precipitation on the membrane; the precipitate subsequently detached itself from the membrane.

At $t = 24$ h, the temperature of the system was increased to 30 °C. Shortly after the increase in temperature, the nickel front was observed to re-enter the cell and retreat to a bed position of approximately 0.275 m. Subsequent increases in temperature resulted in further decreases in the fraction of the bed in the nickel form.

The amount of $Ni(OH)_2$ precipitation was observed to abate after the first increase in temperature. In subsequently regenerated areas of the bed, the precipitate dissolved and the nickel ions were absorbed and transported. The precipitate that had formed in areas of the bed still remained in the nickel form.

The current distribution for each segment pair as a function of time is given in Fig. 5. This figure shows that for each increase in temperature, an increase in the segment's current occurs, particularly for segments at the nickel front. At $t = 24$ h, e.g., the current for segment pairs 1–5 was observed to increase; this was due to the first increase in temperature at that time (25–30 °C). At $t = 48$ h (temperature increases from 30 to 35 °C), the current across pairs 6 and 7 were observed to increase, while the rate of current increase across the fourth segment escalated. The decrease in current for segments 2–6 at $t = 60$ h was due to a decrease in the ambient temperature. At $t = 72$ h, the current across pairs 4–7 were observed to increase after the temperature was changed from 35 to 40 °C. It can be concluded that the

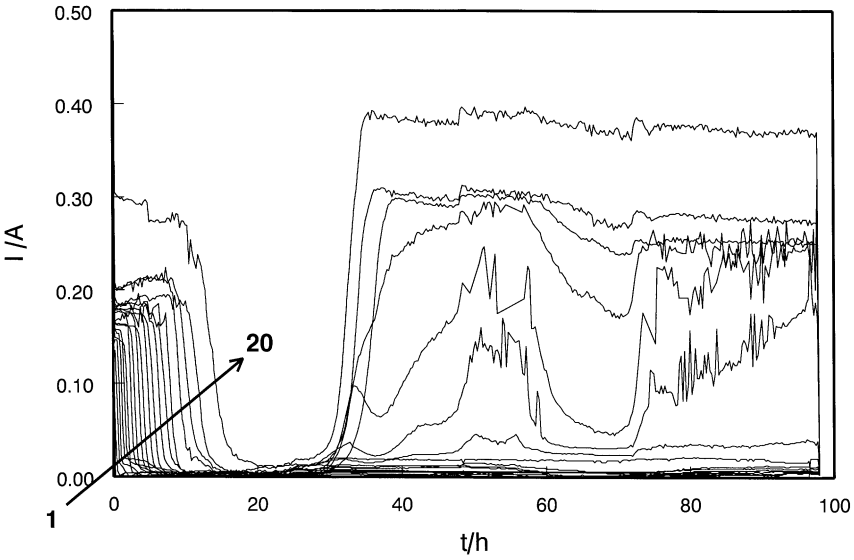

Fig. 5. Current distribution during experiment 2. The feed solution had a nickel concentration of 2 mM and a flow rate of 0.53 $cm^3 s^{-1}$. The temperature was periodically increased. A cell voltage of 5 V was applied. During the first 24 h, the current decreases across each segment in consecutive order. All 20 channels representing the entire cell are depicted.

temperature strongly affects the position of the nickel front and hence the deionization process.

By analysing the current distribution, the position of the nickel front could be obtained. Fig. 6 depicts the position of the tip and base of the front measured from the top of the cell, H_t and H_b, for the first 17 h of experiment 2. During this time the entire bed contained nickel. From this figure, it can be seen that the tip and base leave the bottom of the cell, corresponding to segment pair 20, at approximately $t = 12$ and 17 h, respectively. The dispersion of the front can be expressed as the distance between the tip and base. From Fig. 6, it can be seen that the dispersion of the front increases as it moves further down the column.

The amount of nickel transported to the cathode compartment, $n_{Ni,k}$, is depicted in Fig. 7. Fig. 7 illustrates that during the first 24 h of operation, the flux of nickel into the cell was much greater than the transport of nickel to the cathode compartment, $N_{Ni,k}$. A breakthrough of nickel at the outlet of the central compartment resulted. After the first increase in temperature, the flux of nickel in the bed increased significantly, and after further increases in temperature the $n_{Ni,k}/t$ curve, indicating the quantity of nickel removed from the bed, moves closer to the $n_{Ni,total}/t$ curve indicating the quantity fed to the bed.

No Ni^{2+} was found in the effluent after $t = 24$ h, but it was found in the anolyte. Approximately, 8 mmol of nickel were

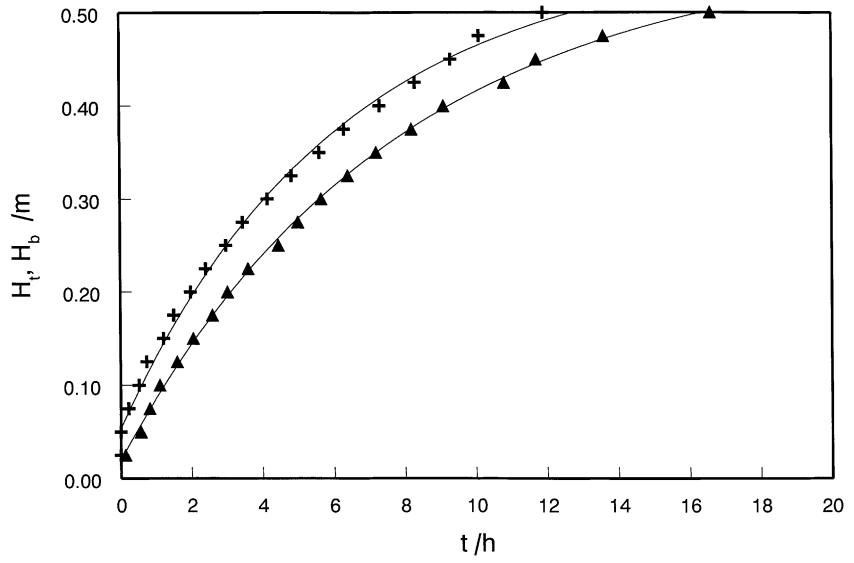

Fig. 6. Position of the tip H_t (+) and base H_b (▲) of the nickel front as a function of time (first 17 h) of experiment 2.

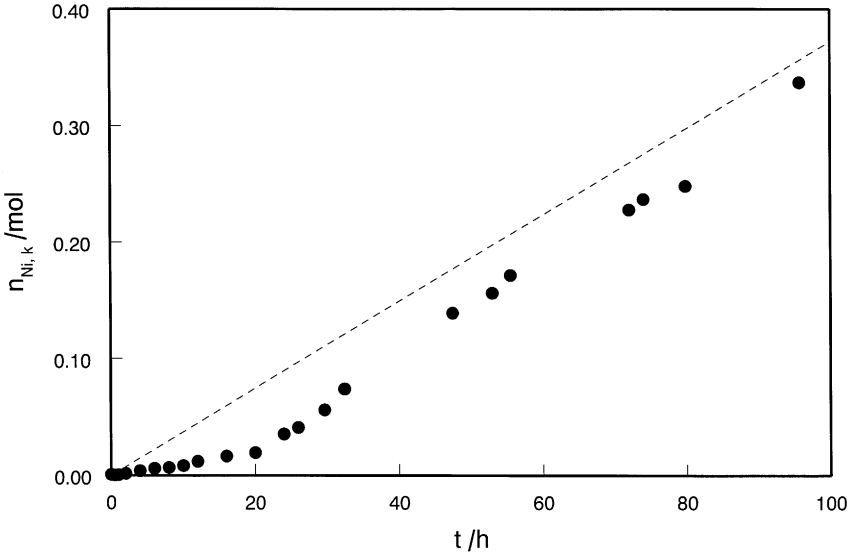

Fig. 7. Quantity of nickel transported to the cathode compartment (●) and the total amount of nickel introduced to the cell during experiment 2 (dashed line).

removed by diffusion to the anode compartment during the entire experiment. The average transport rate of nickel to the anode compartment during the first 24 h, when the system temperature was 25 °C, was found to be 6.67 μmol s^{-1}. This was compared to an average transport rate of 16.7 μmol s^{-1} nickel to the catholyte. The transport of nickel to the anolyte drastically decreased to an average of 0.67 μmol s^{-1}soon after the temperature was increased to 30 °C, while that of the catholyte increased to 66.7 μmol s^{-1}.

The effluent pH during the first 24 h averaged 2.70. This corresponds to a hydrogen concentration of 3.98 mM. During the remainder of the experiment, the pH averaged 2.66 or 4.36 mM H^+. Since all nickel is absorbed after $t = 24$ h, 4 mM of H^+ is produced by the exchange with the 2 mM Ni^{2+} solution fed to the bed; the remainder enters the cell from the outer compartments.

The pressure drop through the centre compartment was observed to decrease as the front moved down the bed. At $t = 0.5$ h, the pressure drop over the entire centre compartment was measured at 3.5×10^4 Pa. It decreased to 3.0×10^4 Pa at $t = 32.5$ h. The decrease in the pressure

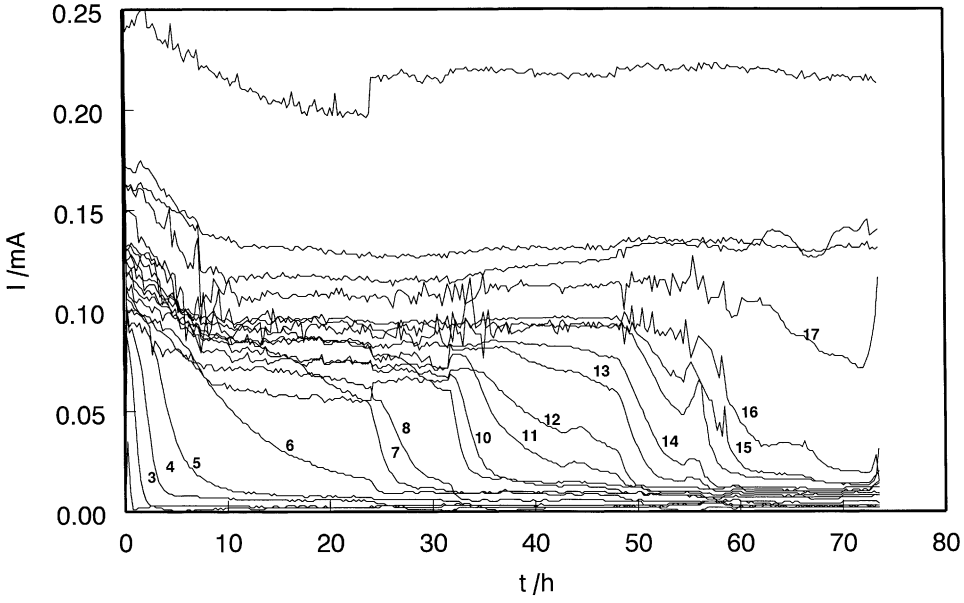

Fig. 8. Current distribution during experiment 3. The feed solution had a nickel concentration of 1 mM. The flow rate was increased periodically from 0.25 to 0.92 cm^3 s^{-1} and the temperature was constant at 25 °C. A cell voltage of 5 V was applied. During the first 24 h, the current decreases across each segment in consecutive order. All 20 channels representing the entire cell are depicted.

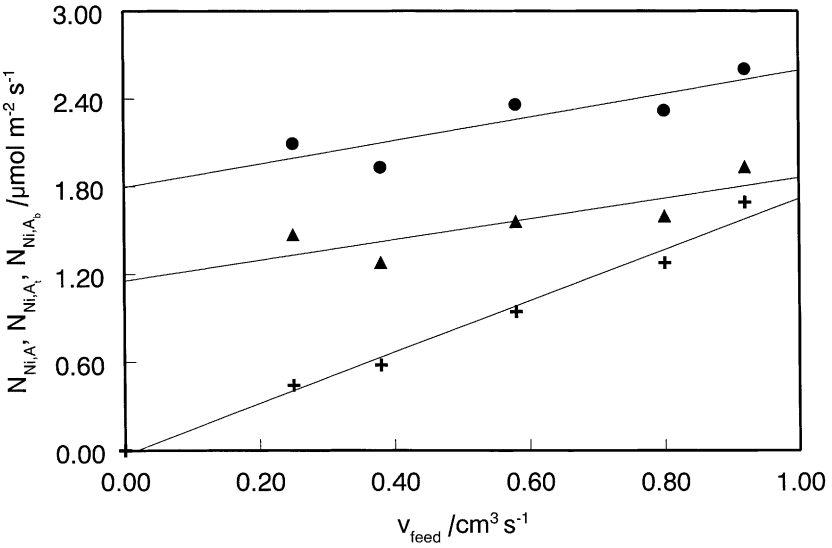

Fig. 9. Flux of nickel into the catholyte as a function of feed solution flow rate. Nickel flux is presented with respect to the area of the bed, A_{bed} (✚), area of the bed until the tip, A_t (●) and base, A_b (▲) of the nickel front.

drop is attributed to the contraction of the bed upon uptake of nickel ions.

3.3. Experiment 3: flow rate variation

During this experiment, the flow rate of the 1 mM $NiSO_4$ feed solution was increased stepwise. After every increase in flow rate the nickel front was observed to move further down the column. The temperature during this experiment was kept constant at 25 °C and no nickel hydroxide precipitation was observed.

The current distribution down the cell is given in Fig. 8. From this data, the location of the tip and base of the nickel front, H_b and H_t, respectively, were plotted for each feed solution flow rate.

The flux of nickel into the catholyte was found to increase after each increase in feed flow rate. Fig. 9 depicts the nickel flux into the catholyte as a function of flow rate. The nickel flux with respect to the entire area of the bed (A_{bed}), the area of the bed until the tip of the nickel front (A_t) and the area until the base of the nickel front (A_b) are depicted. From this figure, it can be seen that the nickel flux with respect to the entire bed increases strongly with flow rate, while the nickel flux with respect to A_t and A_b increased only slightly.

Fig. 10 shows the average concentration of H^+ in the effluent for each flow rate. The concentration of H^+ in the

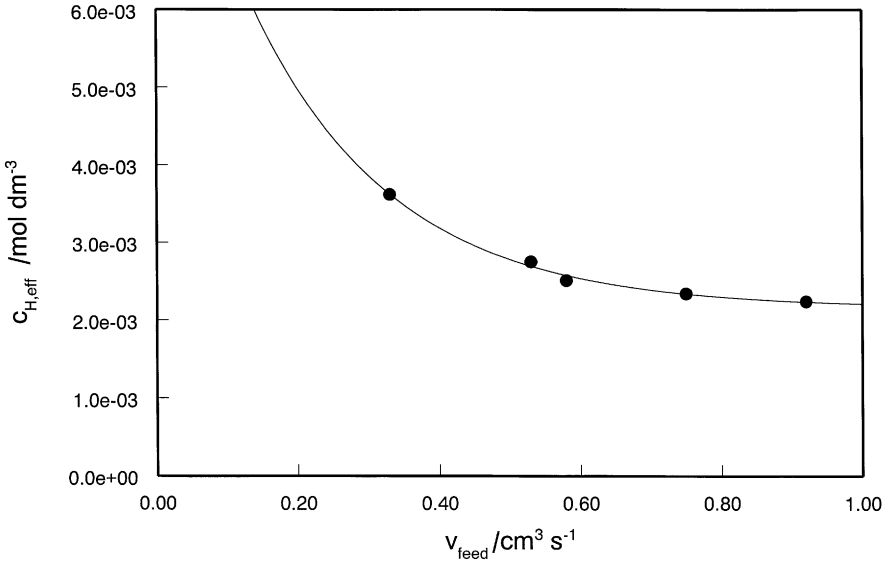

Fig. 10. H^+ concentration in the centre compartment effluent as a function of feed solution flow rate during experiment 3.

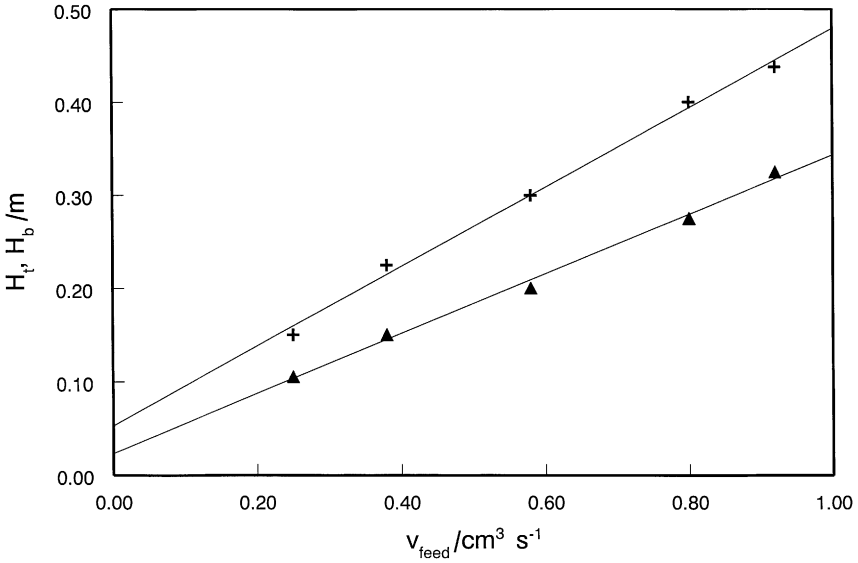

Fig. 11. H_t (✚) and H_b (▲) during experiment 3 as a function of feed solution flow rate.

effluent is seen to decrease exponentially with increasing flow rate. The nickel concentration in the effluent was not detectable with the Flame AAS method used; it was, therefore, below approximately 20 ppb [11].

The development of the nickel front during experiment 3 is depicted in Fig. 11. In this figure, it can be seen that after each increase in flow rate, the nickel front progressed further down the column. It is apparent that the increase in flow rate increased the dispersion of the nickel front. It was found that the current efficiency of the process decreased with increasing solution flow rate.

4. Discussion

The current distribution can be used to track the position of the nickel front. The front stopped when the amount of nickel removed from the bed by migration and diffusion equalled the total amount supplied to the cell

$$n_{\mathrm{Ni,total}} = n_{\mathrm{Ni,bed}} + n_{\mathrm{Ni,k}} + n_{\mathrm{Ni,a}} \quad (1)$$

where 'n' is the quantity in moles, 'k' the cathode compartment, 'a' the anode compartment, 'bed' the packed bed of ion-exchange particles.

The dispersion of the front increased as the front progressed further down the column (Fig. 6). This was especially true when the flow rate of the feed solution was increased (Fig. 11). As both H^+ and Ni^{2+} ions are transported at the nickel front, the efficiency for nickel transport decreases there. The dispersion of the front arises because of Ni^{2+} migration in the interstitial solution towards the cathode, and because nickel ions were only absorbed in regenerated areas of the bed. Since the bed was regenerated from the anode side of the cell, there was a nickel concentration gradient over the bed. Ni^{2+} ions present in the interstitial solution of the bed in the nickel form were not absorbed and thus flowed further down the column. The preferred absorption of nickel along the anode side of the cell and the migration of nickel in the interstitial solution caused the nickel front to elongate along the cathode side of the bed.

The nickel flux into the catholyte during experiment 3 was observed to increase with increasing flow rate. The increase is strong when viewed with respect to the entire bed, but is only slight with respect to the area of the bed in the nickel form (A_b or A_t). The slight increase of the latter is most likely due to the increase in conductivity of the bed upon increasing flow rate. Upon increase in flow rate, the pressure drop over the bed increased, causing the contact area between the particles to increase and, thereby increasing the conductivity of the bed.

The concentration of H^+ in the effluent during all of the experiments was slightly higher than two times the nickel concentration in the feed. This was due to the transport of sulphuric acid from the outer compartments. Fig. 10 shows that the concentration of H^+ in the effluent decreased exponentially with increasing flow rate. When extrapolated to infinite flow rate, the fit from Fig. 10 gives a H^+ concentration in the effluent equal to 2.16 mM; nearly equal to the equivalent concentration of Ni^{2+} in the feed. Hence, the resulting concentration of H^+ in the effluent would be equal to the equivalent concentration of ions exchanged during the process, plus the H^+ ions transported from the outer compartments.

The occurrence of $Ni(OH)_2$ precipitation in experiment 2 showed that its formation during this process depends on the nickel concentration of the feed solution.

Nickel ions were also transported to the anode compartment due to diffusion. The exchange of nickel ions from the highly concentrated resin with protons from the anolyte

took place across the cation-selective membrane. The transport due to diffusion was highest during experiment 2 as the area over which diffusion takes place was greatest during this experiment. At $t = 24$ h, when the temperature of the system was increased to 30 °C from a previous temperature of 25 °C, the flux of nickel to the catholyte increased and a portion of the bed was regenerated to the hydrogen form. At the same time, nickel transport to the anolyte decreased.

The transport of nickel to the anolyte is, therefore, greater when H_b is greater. The volume of the bed in the nickel form increased with increasing nickel concentration in the feed and feed flow solution flow rate and decreased with increasing migration rate of nickel in the system.

5. Conclusions

The purpose of these experiments was to determine the behaviour of a combined electrodialysis/ion-exchange system over a longer time period. By analysing the current distribution during these experiments, the development of the nickel front could be studied. During experiment 1, a pseudo-steady state was obtained in which oscillations in ambient temperature caused oscillations in the nickel flux. Experiment 2 clearly demonstrated the importance of temperature on nickel flux in the ion-exchange bed. It also demonstrated the importance of nickel feed concentration on the formation of nickel hydroxide. The dispersion of the nickel front was shown to increase with feed flow rate during experiment 3. The results showed that the temperature, feed concentration and solution flow rate are all important parameters during the longer term. They were found to affect the flux of nickel to the catholyte, the current efficiency of the process, the volume of resin required for the process as well as the formation of nickel hydroxide in the centre compartment. It has been shown that by controlling these parameters, a continuous process is possible.

References

[1] E. Glueckauf, Brit. Chem. Eng. 4 (1959) 646.
[2] W.R. Walters, D.M. Weiser, L.Y. Marek, Ind. Eng.-Chem. 47 (1955) 61.
[3] V.D. Grebenyuk, N.P. Gnusin, I.B. Barmashenko, A.F. Mazanko, Russ. J. Electrochem. 6 (1970) 139.
[4] H. Neumeister, L. Fürst, R. Flucht, Van Dy Nguyen, Ultrapure Water 13 (1996) 60.
[5] C. Gavach, G. Pourcelly, Separ. Sci. Technol. 34 (1994) 69–84.
[6] G.C. Ganzi, A.D. Jha, F. DiMascio, J.H. Wood, Ultrapure Water 14 (1997) 64–69.
[7] E. Korngold, Desalination 16 (1975) S225.
[8] K. Basta, A. Aliane, A. Lounis, R. Sandeaux, J. Sandeaux, C. Gavach, Desalination 120 (1998) 175–184.
[9] V.D. Grebenyuk, R.D. Chebotareva, N.A. Linkov, V.M. Linkov, Desalination 115 (1998) 255–263.
[10] N.A. Linkov, J.J. Smit, V.M. Linkov, V.D. Grebenyuk, J. Appl. Electrochem. 28 (1998) 1189–1193.
[11] P.B. Spoor, W.R. ter Veen, L.J.J. Janssen, J. Appl. Electrochem. 31 (2001) 523–530.
[12] P.B. Spoor, L.J.J. Janssen, et al., accepted for publication in the Journal of Applied Electrochemistry.
[13] F. Helfferich, Ion Exchange, Dover, New York, 1995.